Available online at www.sciencedirect.com
ScienceDirect
Journal of Magnetism and Magnetic Materials 320 (2008) 2513–2516
Journal of magnetism and magnetic materials
www.elsevier.com/locate/jmmm

Frequency dependence of the ferromagnetic resonance width in magneto-impedance measurements

D. de Cos, A. García-Arribas, J.M. Barandiaran*

Departamento de Electricidad y Electrónica, Facultad de Ciencia y Tecnología, Universidad del País Vasco, P.O. Box 644, 48080 Bilbao, Spain

Available online 4 April 2008

Abstract

Giant magneto-impedance has shown large sensitivities that are of great interest in practical applications. Above certain frequencies the ferromagnetic resonance controls the magneto-impedance behavior, and the resonance width limits the maximum achievable magneto-impedance ratio. In this work we present the evolution of the resonance width as a function of the frequency, determined through magneto-impedance and microwave absorption measurements on a NiFe–Au multilayer thin film. The width of the resonance can be fitted to a curve in the form of $\Delta f \sim f^{-1}$. This is explained by means of a simple model taking into account all inhomogeneities in the sample through a Gaussian distribution of anisotropy fields, as suggested by the shape of the hysteresis loop.

PACS: 74.78.Fk; 75.30.Gw; 76.20.+q; 76.50.+g

Keywords: Magneto-impedance; Ferromagnetic resonance; Anisotropy distribution

1. Introduction

Giant magneto-impedance (GMI) has been actively investigated in recent years [1] for developing high sensitivity magnetic sensors, and some, based on amorphous wires, are already in the market. Miniaturization and electronic integration of GMI devices will however favor thin films and multilayered structures that are increasingly explored [2–4]. The use of such low transverse-dimension samples requires higher operating frequencies because large magneto-impedance (MI) ratio starts when the penetration depth equals the thickness of the sample, at GHz frequencies. While in the past these frequencies were difficult to attain, recent advances in wide consume products offer now high-frequency electronic devices at moderate prices operating at frequencies up to several GHz. However, at these frequencies the magnetization will no longer follow quasi-statically the alternating field associated with the AC sensing current, but precess around the equilibrium position and new phenomena, such as ferromagnetic resonance (FMR), appear. At FMR peaks, the permeability reach much higher values than those in the quasi-static regime, thus setting the maximum theoretical MI ratio achievable [5,6]. The latter is limited by the magnetization damping that should be minimized. Previous works predicted MI ratios as high as 10^4% if normal damping is assumed. Even if the effect of the "exchange conductivity" was taken into account similar figures were obtained.

In this paper we explore the evolution of the damping parameters up to 3 GHz frequency in samples of a previously studied series that gave promising MI values for practical purposes (1260% at 3 GHz) [7]. A simple model based on the distribution of anisotropy fields, modeling all kind of inhomogeneities, is proposed to explain the observed behavior.

2. Experimental

High-frequency impedance measurements have been performed on a NiFe/i/Au/i/NiFe structure. Here /i/ represents an insulating Al_2O_3 layer separating the conductive layers. The multilayered structure is 50 μm wide and 5 mm long and was prepared by sputtering onto a glass

*Corresponding author. Tel.: +34 946012549; fax: +34 946013071.
E-mail address: manub@we.lc.ehu.es (J.M. Barandiaran).

0304-8853/$ - see front matter © 2008 Elsevier B.V. All rights reserved.
doi:10.1016/j.jmmm.2008.04.002

substrate. A magnetic field was applied during the deposition in order to induce a transverse anisotropy. The thicknesses of the different layers are 500 nm for NiFe and Au and 80 nm for Al_2O_3. The deposits were patterned out by photolithographic methods and dry etching. Kerr effect shows that the films present the typical hysteresis loop of transverse anisotropy samples, with an anisotropy field H^K around 500 A/m.

GMI measurements at frequencies up to 3 GHz have been made using techniques described elsewhere [8]. The sample was embedded onto a microstrip line of 50 Ω characteristic impedance. The line was loaded with a precision 50 Ω termination and connected to an Agilent E8358A Network Analyzer. The impedance is obtained from S_{11} parameter measurements after proper calibration and subtraction of the impedance contribution of the test fixture. Care was taken to extract the intrinsic impedance of the trilayer from the microstrip line were it was included. The procedure for that, including an iterative fitting of the line parameters, is described in Refs. [9,10]. The static magnetic field was applied with a pair of Helmholtz coils. Further, microwave power absorption measurements were performed in a magnetic resonance spectrometer working at 9.4 GHz.

3. Results and discussion

Fig. 1 presents the impedance of the sample (real and imaginary parts) as a function of the longitudinally applied magnetic field (H) for two frequencies. At 120 MHz, the impedance presents the typical two peaks shape

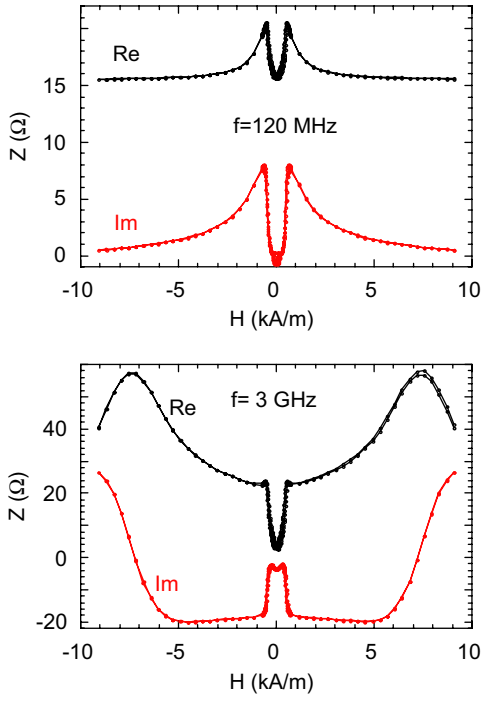

Fig. 1. Magneto-impedance of the trilayer at moderate and high frequency.

corresponding to a transverse anisotropy. These peaks appear at the anisotropy field H^K and are characteristic of the quasi-static magnetization process i.e. the magnetization follows the field at any time.

At 3 GHz FMR takes place as shown by the peaks appearing at high field (variable with the frequency) in Fig. 1b. FMR peaks follow the well-established theory [11], which gives the resonance frequency for an infinite plate as

$$fr = \frac{\mu_0\gamma}{2\pi}\sqrt{(H - H^K)(H + M_S)} \tag{1}$$

where γ is the gyromagnetic ratio, H^K is the anisotropy field and M_S the saturation magnetization. FMR peaks of Fig. 1 fit very well to Eq. (1) using the parameters $\mu_0\gamma/2\pi \approx 35$ kHz/(A/m), $H^K \approx 500$ A/m and $\mu_0 M_S \approx 1.14$ T.

The full description of the resonance must include fitting the full resonance line. The simplest expressions for FMR, is the so-called "transverse permeability" approximation:

$$\mu = \frac{\mu_{DC}}{1 - (f/f_r)^2 + 2j(f\Delta f/f_r^2)} \tag{2}$$

where μ_{DC} is the quasi-static permeability and Δf the line width. By introducing this value into the skin depth, $\delta = \sqrt{2/(\omega\sigma\mu)}$, the impedance of the trilayer can be calculated as that of a single magnetic layer of double thickness $2a$, as $Z = R_{DC}\sqrt{j\theta}\coth(\sqrt{j\theta})$, where $\theta = \sqrt{2}(a/\delta)$.

This is a very good approximation as far as the main contribution to impedance and impedance changes is the resonant permeability of Eq. (2). The contribution of the gold conductor can be accounted for by a slightly different DC conductivity (found by trial and error). Impedance curves as a function of frequency are much more convenient for the fitting in order to keep a constant value of μ_{DC}. Such curves can be easily obtained by cutting the $Z(H)$ ones of Fig. 1 at a constant H.

Fig. 2a shows the fitting of a resonant impedance at a constant applied field from which a value of $\Delta f = 350$ MHz can be obtained. Fig. 2b represents the values for Δf obtained in all the frequency range. The point at 9.4 GHz has been obtained from the field width of the microwave absorption curve "translated" to frequency units by differentiating Eq. (1) as

$$2f(\Delta f) = \mu_0^2(\gamma/2\pi)^2 M_S(\Delta H) \tag{3}$$

By plotting the line width Δf as a function of the resonant frequency (Fig. 2b) we obtain a rather smooth curve that fits a dependence $\Delta f \approx f^{-n}$ with the exponent n close to 1. This plot allows to speculate about the origin of the damping. The "intrinsic" line width used in expression (2) is of course independent of the resonant frequency. Exchange conductivity, on the other hand, gives an $f^{-1/2}$ dependence. None of these mechanisms can explain the large experimental values of Δf, which are almost one order of magnitude higher than the expected value. Sample inhomogeneities, causing the effective field for resonance to vary from point to point, can be at the origin of such values. For instance, magnetic anisotropy dispersion in

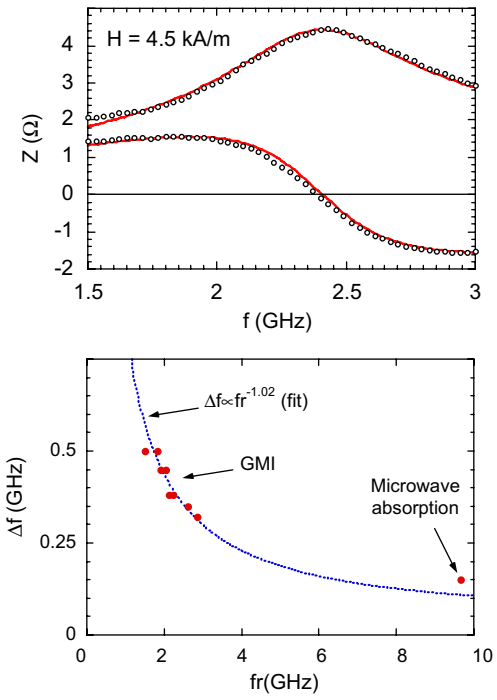

Fig. 2. Fit of the magnetoimpedance to obtain the line width Δf (up) and evolution of this with the resonant frequency (down).

both strength and direction is well documented in amorphous alloys as well as in crystalline thin films. It will add with other contributions in determining the apparent damping of the resonance. Some authors have mentioned that fact, but to date little effort has been paid to quantify it. This is our aim in the present work, as developed in the following section.

4. Damping and dispersion model

We shall model all inhomogeneities in the sample: anisotropy, composition, stresses and roughness giving rise to magnetostatic contributions, and others, as arising from a distribution of anisotropy fields $P(H^K)$.

As a first approximation (Fig. 3a) we take a Gaussian distribution of H^K given by

$$P(H^K) = \frac{1}{\sigma\sqrt{2\pi}} \exp\left(-\frac{(H^K - H_0)^2}{2\sigma^2}\right)$$

where H_0 is the mean anisotropy field and $\Delta H^K = 2\sigma$ can be taken as the width of the anisotropy field distribution. This results in a distribution of resonant frequencies $P(fr)$ linked to the anisotropy field by expression (2), as depicted in Fig. 3b. $P(fr)$ is very asymmetric at low-applied fields, where the resonant frequency is lower. We can define "line width" as the distance in resonant frequency between two elementary peaks separated by ΔH^K (Fig. 4). The plot of Δf as a function of the frequency is very similar to the experimental one (Fig. 2b). In fact the fitting curve used in

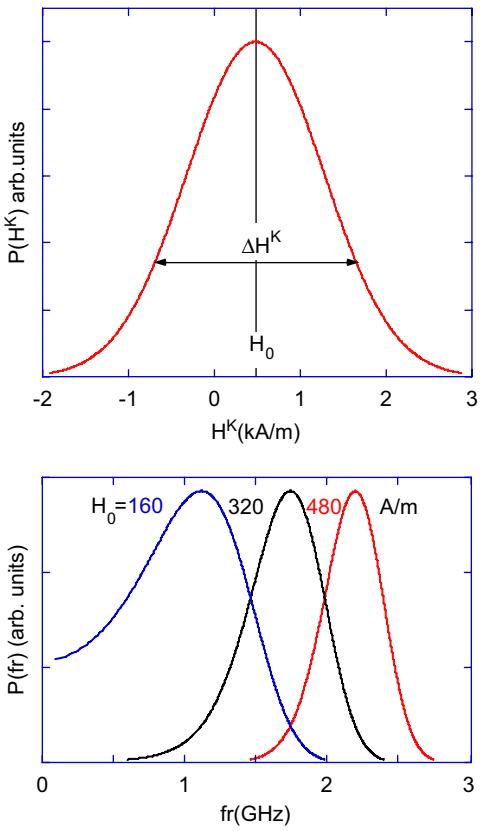

Fig. 3. Distribution of anisotropy fields and resonant frequencies used in the model.

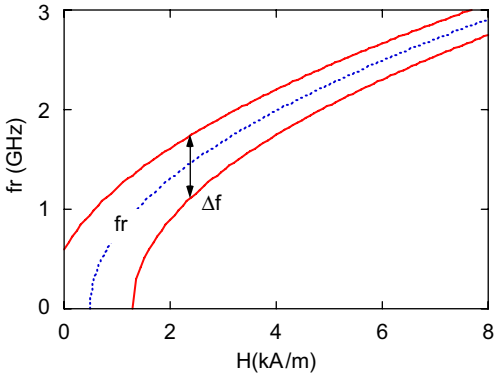

Fig. 4. Evolution of the FMR frequencies as a function of the applied field.

Fig. 2b is just that corresponding to the distribution of H^K used in Figs. 3 and 4, with $H_0 = 500$ A/m and $\sigma = 800$ A/m.

The large spread in H^K needed to fit the experimental curves is somewhat justified by the hysteresis loop of this particular sample, as depicted in Fig. 5. The negative values of H^K do correspond in fact with zones of longitudinal anisotropy or pinning of the magnetization. The large hysteresis and different steps in the magnetization can arise not only from a distribution of induced anisotropies but from a number of different origins, including local demagnetizing factors, but all are well modeled by the

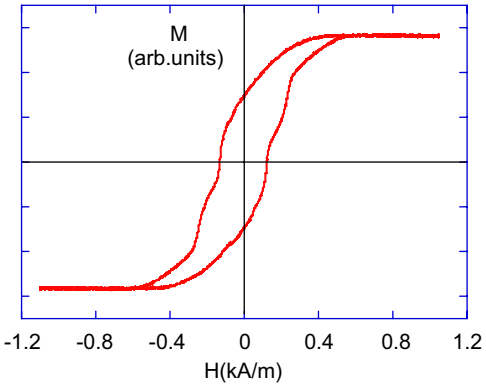

Fig. 5. Hysteresis loop of the trilayer obtained by Kerr effect, reflecting the dispersion in anisotropy.

distribution used. The contribution of all inhomogeneities limits the sharpness of the resonance and lowers the sensitivity of the GMI curves at FMR.

5. Conclusions

MI measurements in a NiFe–Au trilayer are dominated by FMR above 1 GHz. The width of the resonance peaks have been obtained by fitting the GMI curves with the usual transverse permeability expressions from FMR theory, and modeling the inhomogeneities by a distribution of anisotropy fields. The broad resonance peaks, associated with the anisotropy dispersion and other inhomogeneities, lower the sensitivity of the curves, and therefore the optimum GMI device operation.

Acknowledgments

We thank Dr. I. Orue for the Kerr effect measurements. This work was supported partially by the Spanish Ministry of Education and Science under Grant: MAT2005-06806.

References

[1] M. Knobel, L. Kraus, M. Vázquez, in: K.H.J. Buschow (Ed.), Handbook of Magnetic Materials, vol. 15, Elsevier, Amsterdam, 2003, pp. 497–563.
[2] L.V. Panina, K. Mohri, Sensors Actuators A 81 (2000) 71.
[3] D. de Cos, L.V. Panina, N. Fry, I. Orue, A. García Arribas, J.M. Barandiaran, IEEE Trans. Magn. 41 (2005) 3697.
[4] F. Amalou, M.A.M. Gijs, J. Appl. Phys. 95 (2004) 1364.
[5] J.M. Barandiaran, A. García Arribas, J.L. Munoz, G.V. Kulyandskaya, IEEE Trans. Magn. 38 (2002) 3051.
[6] L. Kraus, J. Magn. Magn. Mater. 196–197 (1999) 354.
[7] J.M. Barandiarán, A. García-Arribas, D. de Cos, J. Appl. Phys. 99 (2006) 103904.
[8] D. de Cos, A. García Arribas, M. Barandiaran, Sensors Actuators A 115 (2004) 368.
[9] D. Ménard, M. Britel, P. Ciureanu, A. Yelon, J. Appl. Phys. 81 (1997) 4032.
[10] A. García-Arribas, D. de Cos, J.M. Barandiarán, J. Appl. Phys. 99 (2006) 08C507.
[11] C. Kittel, Introduction to Solid State Physics, seventh ed., Wiley, New York, 1996, p. 505.